Introducing Switched Adaptive Control for Quadrotors for Vertical Operations

by

Viswa Narayan, Spandan Roy

Report No: IIIT/TR/2019/-1

Centre for Robotics
International Institute of Information Technology
Hyderabad - 500 032, INDIA
November 2019

Received: Added at production | Revised: Added at production | Accepted: Added at production

DOI: xxx/xxxx

ARTICLE TYPE

Introducing Switched Adaptive Control for Quadrotors for Vertical Operations†

Viswa N. Sankaranarayanan | Spandan Roy*

[1]Robotics Research Center, International Institute of Information Technology Hyderabad (IIIT-H), Telangana, India

Correspondence
*Spandan Roy, Robotics Research Center, IIIT-H. Email: spandan.roy@iiit.ac.in

Summary

With the advent of intelligent transport, quadrotors are becoming an attractive solution while lifting or dropping of payloads during emergency evacuations, construction works etc. During such operations, dynamic variations in (possibly unknown) payload cause considerable changes in the system dynamics. However, a systematic control solution to tackle such interchanging dynamical behaviour is still missing. This paper proposes a switched dynamical framework to capture the interchanging dynamics of a quadrotor during vertical operations and a robust adaptive control solution to tackle such dynamics when it is unknown. The stability of the closed-loop system is studied analytically and the effectiveness of the proposed solution is verified via simulations.

KEYWORDS:
Adaptive control, switched systems, unknown uncertainty bounds, structural knowledge, quadrotor

1 | INTRODUCTION

Over the past two decades, quadrotors have been a source of considerable research interest owing to its advantages such as simple structure, vertical taking off and landing, rapid maneuvering etc.[1]. Such advantages are crucial in various military and civil applications such as surveillance, fire fighting, environmental monitoring to name a few[2]. Most recently, global research is reorienting toward smart transport systems: relying on its payload carrying capacity, quadrotors are now used in package delivery, construction works, disaster relief operation as a mode of smart aerial transportation[3,4]. An important aspect of such operation is the flexibility of the quadrotor to deal with considerable changes of the system dynamics stemming from dynamically varying payload- called switched dynamics[5]. To illustrate, a motivational example follows:

1.1 | Motivational Example: Dynamic Payload Lifting Operation

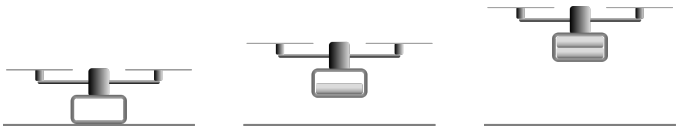

FIGURE 1 A schematic representing a quadrotor ascending with dynamic payload.

†

In a typical construction assignment or emergency evacuation, a quadrotor might be required to lift or drop varying payload (construction and disaster relief materials). Dynamic variation in payload may be orchestrated from situations such as an emergency evacuation from a high rise building, where humans are rescued from various floors. One such lifting operation is sketched in Fig. 1 via three phases: (i) in the first phase, the quadrotor rests on the ground without any payload; (ii) in the second phase, it starts to ascend with an initial payload; (iii) and in the third phase, a new payload is attached to the quadrotor as it ascends to its desired height. Similar phases can be observed during a construction scenario. In a reverse scenario to Fig. 1, a quadrotor may descend from a height while releasing payloads at different heights (e.g., dropping/throwing fire extinguishing materials at different floors). Clearly, the overall mass/inertia of the quadrotor changes (switches) during the interchange of these phases. Currently, to the best of the authors' knowledge, no control solution exists to tackle the interchanging dynamics of a quadrotor during the aforementioned scenarios. In the following, attempts in this direction are discussed, together with the contribution brought by this research.

1.2 | Related Works and Contribution

In the quest to operate a quadrotor under various sources of parametric uncertainty, the control regime, after initial model based designs (cf. the survey paper[6] for the evolutions of various designs), has inevitably moved to some notable adaptive control works[4,7–14]. However, no adaptive design addresses the issue of switched dynamics as discussed earlier. On the other hand, extending these works to a switched dynamics scenario would rely on finding a common Lyapunov function, which again is difficult (if at all possible) to achieve in practical systems[15].

Therefore, a relevant question arises whether the existing switched adaptive control designs[15–23] (and references therein) can be applied to a switched quadrotor system while carrying uncertain (and possibly unknown) payload. Unfortunately, to the best of the authors' knowledge, existing literature does not present a positive answer to this: though[22,23] do not rely on the structure of system dynamics in contrast to the state of the art, they still require bound knowledge of the uncertain mass/inertia matrix (in the context of electro-mechanical systems) either to design control law[23] or switching law[22].

In light of the above discussions, an adaptive switched framework that can tackle completely unknown dynamics of quadrotor in a swithced dynamics setting is still missing. Toward this direction, the proposed switched adaptive solution has the following major contributions:

- A switched dynamics for quadrotor is formulated which suitably represents the changing dynamics during a vertical (lifting/dropping) operation under dynamic variation of payload.
- Compared to the state-of-the-art, the proposed adaptive law and switching law do not require any a priori knowledge of the system dynamics parameters and payload. Further, differently from[7,11], the effects of cross-coupling terms arising from the lateral motion are considered as state-dependent uncertainty.

Note that in this work, the external payloads are considered to be rigidly attached to the quadrotor platform; suspended payload requires separate design in the framework of underactuation and can be considered as a future work. The rest of the paper is organized as follows: Section 2 describes the switched quadrotor systems and highlights various issues in the state of the art; Section 3 details the proposed control framework, while the corresponding stability analysis is carried out in Section 4; a simulation study is provided in Section 5, while Section 6 presents the concluding remarks.

The following notations are used throughout the paper: $\lambda_{\min}(\bullet)$ and $||\bullet||$ represent minimum eigenvalue and Euclidean norm of $(\bullet)$ respectively; $\mathbf{I}$ denotes identity matrix with appropriate dimension.

2 | SYSTEM DYNAMICS AND PROBLEM FORMULATION

During a vertical operation, a quadrotor needs to maintain a given (possibly time-varying) height (z) and attitude (ϕ, φ, ψ), at a fixed (x, y) position. Under such scenario and based on the dynamics structure as in (A3) (cf. Appendix for details), a switched quadrotor dynamics (cf. Fig. 2) for vertical operations can be represented in Earth-fixed frame $\{X_W, Y_W, Z_W\}$ as

$$\mathbf{M}_\sigma(\mathbf{q})\ddot{\mathbf{q}} + \mathbf{C}_\sigma(\mathbf{q}, \dot{\mathbf{q}})\dot{\mathbf{q}} + \mathbf{G}_\sigma(\mathbf{q}) + \mathbf{H}_\sigma(\mathbf{q})\ddot{\mathbf{q}}_\mathbf{u} + \mathbf{d}_\sigma = \boldsymbol{\tau}_\sigma, \tag{1}$$

where $\mathbf{q} = \{z, \phi, \varphi, \psi\}$ and $\mathbf{q_u} = \{x, y\}$ (ω_i in Fig. 2 is the angular velocity of the i^{th} rotor); for each subsystem σ, $\mathbf{M_\sigma}(\mathbf{q}) \in \mathbb{R}^{4\times4}$ is the mass/inertia matrix; $\mathbf{C}_\sigma(\mathbf{q}, \dot{\mathbf{q}}) \in \mathbb{R}^{4\times4}$ denote the Coriolis, centripetal terms; $\mathbf{G}_\sigma(\mathbf{q}) \in \mathbb{R}^4$ denotes the gravity vector;

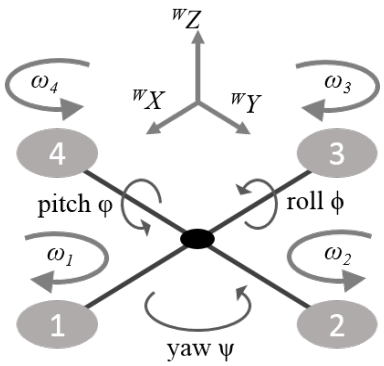

FIGURE 2 Coordinates of a quadrotor.

$\mathbf{H}_\sigma(\mathbf{q})\ddot{\mathbf{q}}_\mathbf{u} \in \mathbb{R}^4$ represents the vector of cross-coupling terms stemming from (x, y) sub-dynamics; $\mathbf{d}_\sigma(t) \in \mathbb{R}^4$ denotes bounded external disturbance and $\boldsymbol{\tau}_\sigma \in \mathbb{R}^4$ is the control input. The mapping from $\boldsymbol{\tau}$ to thrust and torques of individual motors are well reported in literature (cf.[3] and references therein).

Here $\sigma(t) : [0\ \infty) \mapsto \Omega$ is a piecewise constant function of time, called the switching signal, taking values in $\Omega = \{1, 2, \cdots, N\}$. The following class of slowly-switching signals is considered:

Definition 1. Average Dwell Time (ADT)[24]: For a switching signal $\sigma(t)$ and each $t_2 \geq t_1 \geq 0$, let $N_\sigma(t_1, t_2)$ denote the number of discontinuities in the interval $[t_1, t_2)$. Then $\sigma(t)$ has an average dwell time ϑ if for a given scalar $N_0 > 0$

$$N_\sigma(t_1, t_2) \leq N_0 + (t_2 - t_1)/\vartheta, \ \ \forall t_2 \geq t_1 \geq 0$$

where N_0 is termed as chatter bound.

As the quadrotor dynamics (1) follows the celebrated Euler-Lagrange dynamics formulation[3], each subsystem in (1) presents a few interesting properties (cf.[25]), which are later exploited for control design as well as stability analysis:
Property 1: $\exists \overline{c}_\sigma, \overline{g}_\sigma, \overline{h}_\sigma, \overline{d}_\sigma \in \mathbb{R}^+$ such that $||\mathbf{C}_\sigma(\mathbf{q}, \dot{\mathbf{q}})|| \leq \overline{c}_\sigma||\dot{\mathbf{q}}||$, $||\mathbf{G}_\sigma(\mathbf{q})|| \leq \overline{g}_\sigma$, $||\mathbf{H}_\sigma(\mathbf{q})|| \leq \overline{h}_\sigma$ and $||\mathbf{d}_\sigma(t)|| \leq \overline{d}_\sigma$.
Property 2: The matrix $\mathbf{M}_\sigma(\mathbf{q})$ is symmetric and uniformly positive definite $\forall \mathbf{q}$, implying that $\exists \underline{m}_\sigma, \overline{m}_\sigma \in \mathbb{R}^+$ such that

$$0 < \underline{m}_\sigma \mathbf{I} \leq \mathbf{M}_\sigma(\mathbf{q}) \leq \overline{m}_\sigma \mathbf{I}. \tag{2}$$

A few remarks regarding system (1) follow, which aid in designing the proposed switching control.

Remark 1. (Uncertainty). As a design challenge, the switched system (1) is considered to be unknown in the sense that the knowledge of $\mathbf{M}_\sigma, \mathbf{C}_\sigma, \mathbf{H}_\sigma, \mathbf{G}_\sigma, \mathbf{d}_\sigma$ and their corresponding bounds, i.e., $\underline{m}_\sigma, \overline{m}_\sigma, \overline{c}_\sigma, \overline{g}_\sigma, \overline{h}_\sigma, \overline{d}_\sigma$ are *completely unknown*.

Remark 2. (Collocated Design). Note that a quadrotor dynamics is essentially underactuated, where x and y positions represent the nonactuated coordinates. During a vertical operation (i.e., a near hovering condition), there exist time-scale separation between (z, ϕ, φ, ψ) and (x, y) dynamics, where the former evolves faster than the later[9]. Therefore, it is standard to track only the actuated coordinates (z, ϕ, φ, ψ) of a quadrotor during such operation[7,11]. In the literature of underactuated systems, such control design, i.e., tracking of only actuated coordinates, is called *collocated design* (cf.[26,27]). A simultaneous switched tracking controller for all the actuated and non-actuated coordinates, in line with[28], can also be a challenging future work.

Remark 3. (Cross-coupling terms). Notwithstanding slow evolution of the lateral (i.e., (x, y)) motion compared to the vertical (z) and attitude (ϕ, φ, ψ) motions due to time-scale separation, ignoring its effect is conservative: especially, variation in payload and perturbation in attitude may cause some lateral motion, affecting $\mathbf{q}$. Therefore, differently form[7,11], the cross-coupling term $\mathbf{H}_\sigma(\mathbf{q})\ddot{\mathbf{q}}_\mathbf{u}$ is considered in (1), where $\mathbf{H}_\sigma(\mathbf{q})$ captures the effects of variations in payload and attitude (cf. Appendix).

Control Problem: Under Properties 1 and 2, the control problem is to design a switched adaptive (collocated) control framework for a vertical operation of a quadrotor following the dynamics (1), without any knowledge of system parameters (in line with Remark 1).

The following section solves this control problem.

3 | SWITCHED CONTROLLER DESIGN

Assumption 1 ([29,30]). The desired trajectories satisfy $\mathbf{q}^d, \dot{\mathbf{q}}^d, \ddot{\mathbf{q}}^d \in \mathcal{L}_\infty$. Furthermore, $\mathbf{q}, \dot{\mathbf{q}}, \ddot{\mathbf{q}}$ are available for feedback.

For control design purposes, the dynamics (1) is re-arranged as

$$\mathbf{D}_\sigma \ddot{\mathbf{q}} + \mathbf{E}_\sigma(\mathbf{q}, \dot{\mathbf{q}}, \ddot{\mathbf{q}}, \ddot{\mathbf{q}}_\mathbf{u}, t) = \boldsymbol{\tau}_\sigma, \tag{3}$$

which has been obtained by adding and subtracting $\mathbf{D}_\sigma \ddot{\mathbf{q}}$ to (1), where $\mathbf{D}_\sigma$ is a user-defined constant positive definite matrix and $\mathbf{E}_\sigma \triangleq (\mathbf{M}_\sigma - \mathbf{D}_\sigma)\ddot{\mathbf{q}} + \mathbf{C}_\sigma \dot{\mathbf{q}} + \mathbf{G}_\sigma + \mathbf{H}_\sigma \ddot{\mathbf{q}}_\mathbf{u} + \mathbf{d}_\sigma$. The selection of $\mathbf{D}_\sigma$ would be discussed later (cf. Remark 5).

Let $\mathbf{e}(t) \triangleq \mathbf{q}(t) - \mathbf{q}^d(t)$ be the tracking error, $\boldsymbol{\xi}(t) \triangleq [\mathbf{e}(t),\ \dot{\mathbf{e}}(t)]$ and $\mathbf{r}_\sigma$ be the filtered tracking error variable defined as

$$\mathbf{r}_\sigma \triangleq \mathbf{B}^T \mathbf{P}_\sigma \boldsymbol{\xi}, \qquad \sigma \in \Omega \tag{4}$$

where $\mathbf{P}_\sigma > \mathbf{0}$ is the solution to the Lyapunov equation $\mathbf{A}_\sigma^T \mathbf{P}_\sigma + \mathbf{P}_\sigma \mathbf{A}_\sigma = -\mathbf{Q}_\sigma$ for some $\mathbf{Q}_\sigma > \mathbf{0}$, $\mathbf{A}_\sigma \triangleq \begin{bmatrix} \mathbf{0} & \mathbf{I} \\ -\mathbf{K}_{1\sigma} & -\mathbf{K}_{2\sigma} \end{bmatrix}$ and $\mathbf{B} \triangleq \begin{bmatrix} \mathbf{0} & \mathbf{I} \end{bmatrix}^T$. Here, $\mathbf{K}_{1\sigma}$ and $\mathbf{K}_{2\sigma}$, where $\sigma \in \Omega$, are two user-defined positive definite gain matrices and their positive definiteness guarantees that $\mathbf{A}_\sigma$ is Hurwitz.

The control law is designed as

$$\boldsymbol{\tau}_\sigma = \mathbf{D}_\sigma(-\boldsymbol{\Lambda}_\sigma \boldsymbol{\xi} - \Delta\boldsymbol{\tau}_\sigma + \ddot{\mathbf{q}}^d), \tag{5a}$$

$$\Delta\boldsymbol{\tau}_\sigma = \begin{cases} \rho_\sigma \frac{\mathbf{r}_\sigma}{||\mathbf{r}_\sigma||} & \text{if } ||\mathbf{r}_\sigma|| \geq \varpi \\ \rho_\sigma \frac{\mathbf{r}_\sigma}{\varpi} & \text{if } ||\mathbf{r}_\sigma|| < \varpi \end{cases}, \tag{5b}$$

where $\boldsymbol{\Lambda}_\sigma \triangleq [\mathbf{K}_{1\sigma}\ \mathbf{K}_{2\sigma}]$; $\varpi > 0$ is a user-defined scalar to avoid chattering and the design of ρ_σ will be discussed later. Substituting (5a) in (3) yields

$$\ddot{\mathbf{e}} = -\boldsymbol{\Lambda}_\sigma \boldsymbol{\xi} - \Delta\boldsymbol{\tau}_\sigma + \chi_\sigma, \tag{6}$$

where $\chi_\sigma \triangleq -\mathbf{D}_\sigma^{-1}\mathbf{E}_\sigma$ is defined as the *overall uncertainty*. Using Properties 1, 2 and Assumption 1 one can verify that

$$||\chi_\sigma|| \leq \theta_{0\sigma}^* + \theta_{1\sigma}^* ||\boldsymbol{\xi}|| + \theta_{2\sigma}^* ||\boldsymbol{\xi}||^2 + \theta_{3\sigma}^* ||\ddot{\overline{\mathbf{q}}}|| \triangleq \mathbf{Y}_\sigma^T \boldsymbol{\Theta}_\sigma^*, \tag{7}$$

where $\overline{\mathbf{q}} = [\mathbf{q}^T\ \mathbf{q}_\mathbf{u}^T]^T$; $\mathbf{Y}_\sigma = [1\ ||\boldsymbol{\xi}||\ ||\boldsymbol{\xi}||^2\ ||\ddot{\overline{\mathbf{q}}}||]^T$ and $\boldsymbol{\Theta}_\sigma^* = [\theta_{0\sigma}^*\ \theta_{1\sigma}^*\ \theta_{2\sigma}^*\ \theta_{3\sigma}^*]^T$. The scalars $\theta_{i\sigma}^* \in \mathbb{R}^+$ $i = 0, \cdots, 3$ are unknown $\forall \sigma \in \Omega$ and they are defined as

$$\begin{aligned} \theta_{0\sigma}^* &= ||\mathbf{D}_\sigma^{-1}||(\overline{g}_\sigma + \overline{d}_\sigma + \overline{c}_\sigma ||\dot{\mathbf{q}}^d||^2), \\ \theta_{1\sigma}^* &= 2\overline{c}_\sigma ||\mathbf{D}_\sigma^{-1}|| ||\dot{\mathbf{q}}^d||, \\ \theta_{2\sigma}^* &= \overline{c}_\sigma ||\mathbf{D}_\sigma^{-1}||, \\ \theta_{3\sigma}^* &= ||\mathbf{D}_\sigma^{-1}\mathbf{M}_\sigma - \mathbf{I}|| + ||\mathbf{D}_\sigma^{-1}||\overline{h}. \end{aligned}$$

The upper bound structure (7) is obtained by using the following relations $\mathbf{q} = \mathbf{e} + \mathbf{q}^d$, $\dot{\mathbf{q}} = \dot{\mathbf{e}} + \dot{\mathbf{q}}^d$, $||\boldsymbol{\xi}|| \geq ||\mathbf{e}||$ and $||\boldsymbol{\xi}|| \geq ||\dot{\mathbf{e}}||$ (cf. [31,32] for details).

Based on the upper bound structure in (7), the gain ρ_σ in (5a) is designed as

$$\begin{aligned} \rho_\sigma &= \hat{\theta}_{0\sigma} + \hat{\theta}_{1\sigma} ||\boldsymbol{\xi}|| + \hat{\theta}_{2\sigma} ||\boldsymbol{\xi}||^2 + \hat{\theta}_{3\sigma} ||\ddot{\overline{\mathbf{q}}}|| + \zeta_\sigma + \gamma_\sigma \\ &\triangleq \mathbf{Y}_\sigma^T \hat{\boldsymbol{\Theta}}_\sigma + \zeta_\sigma + \gamma_\sigma, \end{aligned} \tag{8}$$

where $\hat{\mathbf{\Theta}}_\sigma \triangleq [\hat{\theta}_{0\sigma}\ \hat{\theta}_{1\sigma}\ \hat{\theta}_{2\sigma}\ \hat{\theta}_{3\sigma}]^T$ and $\zeta_\sigma, \gamma_\sigma$ are auxiliary gains needed for closed-loop stabilization. Defining $\varrho_\sigma \triangleq (\lambda_{\min}(\mathbf{Q}_\sigma)/\lambda_{\max}(\mathbf{P}_\sigma))$, the gains $\hat{\theta}_{i\sigma}, \zeta_\sigma$ and γ_σ are adapted using the following laws:

$$\dot{\hat{\theta}}_{jp} = ||\mathbf{r}_p||||\boldsymbol{\xi}||^j - \alpha_{jp}\hat{\theta}_{jp},\ \dot{\hat{\theta}}_{j\overline{p}} = 0,\ j = 0, 1, 2 \tag{9a}$$

$$\dot{\hat{\theta}}_{3p} = ||\mathbf{r}_p||||\ddot{\overline{\mathbf{q}}}|| - \alpha_{3p}\hat{\theta}_{3p},\ \dot{\hat{\theta}}_{3\overline{p}} = 0 \tag{9b}$$

$$\dot{\zeta}_p = -\left(1 + \hat{\theta}_{3p}||\ddot{\overline{\mathbf{q}}}|||\mathbf{r}_p||\right)\zeta_p + \bar{\epsilon}_p,\ \dot{\zeta}_{\overline{p}} = 0, \tag{9c}$$

$$\dot{\gamma}_p = 0,\ \dot{\gamma}_{\overline{p}} = -\left(1 + \frac{\varrho_{\overline{p}}}{2}\sum_{i=0}^{3}\hat{\theta}_{i\overline{p}}^2\right)\gamma_{\overline{p}} + \epsilon_{\overline{p}}, \tag{9d}$$

$$\text{with } \alpha_{i\sigma} > \varrho_\sigma/2,\ i = 0, 1, 2, 3, \tag{9e}$$

$$\hat{\theta}_{i\sigma}(t_0) > 0,\ \zeta_\sigma(t_0) = \bar{\zeta}_\sigma > \bar{\epsilon}_\sigma,\ \gamma_\sigma(t_0) = \bar{\gamma}_\sigma > \epsilon_\sigma, \tag{9f}$$

where p and $\overline{p} \in \Omega\backslash\{p\}$ denote the active and inactive subsystems respectively; $\alpha_{ip}, \bar{\epsilon}_p, \epsilon_{\overline{p}} \in \mathbb{R}^+$ are static design scalars and t_0 is the initial time.

We define $\varrho_{M\sigma} \triangleq \lambda_{\max}(\mathbf{P}_\sigma)$, $\varrho_{m\sigma} \triangleq \lambda_{\min}(\mathbf{P}_\sigma)$, $\bar{\varrho}_M \triangleq \max_{\sigma\in\Omega}(\varrho_{M\sigma})$ and $\underline{\varrho}_m \triangleq \min_{\sigma\in\Omega}(\varrho_{m\sigma})$. Following Definition 1 of ADT[24], the switching law is proposed as

$$\vartheta > \vartheta^* = \ln\mu/\kappa, \tag{10}$$

where $\mu \triangleq \bar{\varrho}_M/\underline{\varrho}_m$; κ is a scalar defined as $0 < \kappa < \varrho$ where $\varrho \triangleq \min_{\sigma\in\Omega}(\lambda_{\min}(\mathbf{Q}_\sigma)/\lambda_{\max}(\mathbf{P}_\sigma))$.

Remark 4. (On the use of acceleration measurements). Being primarily intended for outdoor applications, use of inertial navigation systems with accelerometers are quite common for quadrotor systems [10,33]. Intial pioneering adaptive control designs for (non-switched) systems made use of acceleration measurements [30], which was later avoided due to want of sensors. Nevertheless, with the technological advancements and with cheaper prices, usage of acceleration feedback can be found nowadays in many (non-switched) robust and adaptive designs (cf. [29,32,34,35] and references therein).

4 | STABILITY ANALYSIS OF THE PROPOSED CONTROLLER

Theorem 1. Under Assumption 1 and Properties 1-2, the closed-loop trajectories of system (6) employing the control laws (5) and (8) with adaptive law (9) and switching law (10) are Uniformly Ultimately Bounded (UUB). An ultimate bound b on the tracking error $\boldsymbol{\xi}$ can be found as

$$b = \sqrt{\frac{2\bar{\varrho}_M^{(N_0+1)}\left(\delta + \varpi\delta_1\right)}{\underline{\varrho}_m^{(N_0+2)}\left(\varrho - \kappa\right)}}, \tag{11}$$

where the scalars δ and δ_1 are defined during the proof.

Proof. From (9a)-(9d) and the initial conditions (9f), it can be verified that $\exists\underline{\zeta}_\sigma, \underline{\gamma}_\sigma \in \mathbb{R}^+$ such that

$$\begin{aligned}\hat{\theta}_{i\sigma}(t) \geq 0,\ 0 < \underline{\zeta}_\sigma \leq \zeta_\sigma(t) \leq \bar{\zeta}_\sigma,\\ \text{and } 0 < \underline{\gamma}_\sigma \leq \gamma_\sigma(t) \leq \bar{\gamma}_\sigma\ \ \forall t \geq t_0.\end{aligned} \tag{12}$$

Stability analysis is carried out based on the multiple Lyapunov candidate:

$$V = \frac{1}{2}\boldsymbol{\xi}^T\mathbf{P}_\sigma\boldsymbol{\xi} + \sum_{s=1}^{N}\sum_{i=0}^{3}\frac{(\hat{\theta}_{is} - \theta_{is}^*)^2}{2} + \frac{\gamma_s}{\underline{\gamma}} + \frac{\zeta_s}{\underline{\zeta}}, \tag{13}$$

where $\underline{\gamma} = \min_{s\in\Omega}(\underline{\gamma}_s)$ and $\underline{\zeta} = \min_{s\in\Omega}(\underline{\zeta}_s)$. Observing that $\boldsymbol{\Lambda}_\sigma\boldsymbol{\xi} = \mathbf{K}_{1\sigma}\mathbf{e} + \mathbf{K}_{2\sigma}\dot{\mathbf{e}}$, the error dynamics obtained in (6) becomes

$$\dot{\boldsymbol{\xi}} = \mathbf{A}_\sigma\boldsymbol{\xi} + \mathbf{B}\left(\boldsymbol{\chi}_\sigma - \Delta\boldsymbol{\tau}_\sigma\right). \tag{14}$$

Note that $V(t)$ might be discontinuous at the switching instants and only remains continuous during the time interval between two consecutive switchings. Without loss of generality, the behaviour of V is studied at the switching instant $t_{l+1},\ l \in \mathbb{N}^+$. Let

an active subsystem be $\sigma(t_{l+1}^-)$ when $t \in [t_l \;\; t_{l+1})$ and $\sigma(t_{l+1})$ when $t \in [t_{l+1} \;\; t_{l+2})$. We have before and after switching

$$\begin{aligned}
V(t_{l+1}^-) &= \frac{1}{2}\xi^T(t_{l+1}^-)\mathbf{P}_{\sigma(t_{l+1}^-)}\xi(t_{l+1}^-) \\
&\quad + \sum_{s=1}^{N}\sum_{i=0}^{3}\left\{\frac{(\hat{\theta}_{is}(t_{l+1}^-) - \theta_{is}^*)^2}{2} + \frac{\gamma_s(t_{l+1}^-)}{\underline{\gamma}} + \frac{\zeta_s(t_{l+1}^-)}{\underline{\zeta}}\right\}, \\
V(t_{l+1}) &= \frac{1}{2}\xi^T(t_{l+1})\mathbf{P}_{\sigma(t_{l+1})}\xi(t_{l+1}) \\
&\quad + \sum_{s=1}^{N}\sum_{i=0}^{3}\left\{\frac{(\hat{\theta}_{is}(t_{l+1}) - \theta_{is}^*)^2}{2} + \frac{\gamma_s(t_{l+1})}{\underline{\gamma}} + \frac{\zeta_s(t_{l+1})}{\underline{\zeta}}\right\},
\end{aligned}$$

respectively. Thanks to the continuity of the tracking error $\boldsymbol{\xi}$ in (14) and of the gains $\hat{\theta}_{i\sigma}$, ζ_σ and γ_σ in (9), we have $\boldsymbol{\xi}(t_{l+1}^-) = \boldsymbol{\xi}(t_{l+1})$, $(\hat{\theta}_{is}(t_{l+1}^-) - \theta_{is}^*) = (\hat{\theta}_{is}(t_{l+1}) - \theta_{is}^*)$, $\gamma_s(t_{l+1}^-) = \gamma_s(t_{l+1})$ and $\zeta_s(t_{l+1}^-) = \zeta_s(t_{l+1})$. Further, owing to the facts $\boldsymbol{\xi}^T(t)\mathbf{P}_{\sigma(t)}\boldsymbol{\xi}(t) \leq \bar{\varrho}_M\boldsymbol{\xi}^T(t)\boldsymbol{\xi}(t)$ and $\boldsymbol{\xi}^T(t)\mathbf{P}_{\sigma(t)}\boldsymbol{\xi}(t) \geq \underline{\varrho}_m\boldsymbol{\xi}^T(t)\boldsymbol{\xi}(t)$, one has

$$\begin{aligned}
V(t_{l+1}) - V(t_{l+1}^-) &= \frac{1}{2}\boldsymbol{\xi}^T(t_{l+1})(\mathbf{P}_{\sigma(t_{l+1})} - \mathbf{P}_{\sigma(t_{l+1}^-)})\boldsymbol{\xi}(t_{l+1}) \\
&\leq \frac{\bar{\varrho}_M - \underline{\varrho}_m}{2\underline{\varrho}_m}\boldsymbol{\xi}^T(t_{l+1})\mathbf{P}_{\sigma(t_{l+1}^-)}\boldsymbol{\xi}(t_{l+1}) \\
&\leq \frac{\bar{\varrho}_M - \underline{\varrho}_m}{\underline{\varrho}_m}V(t_{l+1}^-) \\
\Rightarrow V(t_{l+1}) &\leq \mu V(t_{l+1}^-),
\end{aligned} \tag{15}$$

with $\mu = \bar{\varrho}_M/\underline{\varrho}_m \geq 1$. At this point, the behaviour of $V(t)$ between two consecutive switching instants, i.e., when $t \in [t_l \;\; t_{l+1})$ can be studied.

We shall proceed the stability analysis for the two cases (i) $||\mathbf{r}_\sigma|| \geq \varpi$ and (ii) $||\mathbf{r}_\sigma|| < \varpi$ using the Lyapunov function (13). For convenience of notation, let us denote the active subsystem $\sigma(t_{l+1}^-)$ with p and any inactive subsystem with $\overline{p}$.

Case (i) $||\mathbf{r}_\sigma|| \geq \varpi$

Using (7), (14), (9) and the Lyapunov equation $\mathbf{A}_p^T\mathbf{P}_p + \mathbf{P}_p\mathbf{A}_p = -\mathbf{Q}_p$, the time derivative of (13) yields

$$\begin{aligned}
\dot{V} &= \frac{1}{2}\boldsymbol{\xi}^T(\mathbf{A}_p^T\mathbf{P}_p + \mathbf{P}_p\mathbf{A}_p)\boldsymbol{\xi} + \boldsymbol{\xi}^T\mathbf{P}_p\mathbf{B}\left(\chi_p - \rho_p\frac{\mathbf{r}_p}{||\mathbf{r}_p||}\right) \\
&\quad + \sum_{s=1}^{N}\sum_{i=0}^{3}\left\{(\hat{\theta}_{is} - \theta_{is}^*)\dot{\hat{\theta}}_{is} + \frac{\dot{\gamma}_s}{\underline{\gamma}} + \frac{\dot{\zeta}_s}{\underline{\zeta}}\right\} \\
&\leq -\frac{1}{2}\boldsymbol{\xi}^T\mathbf{Q}_p\boldsymbol{\xi} + ||\chi_p||||\mathbf{r}_p|| - \rho_p||\mathbf{r}_p|| \\
&\quad + \sum_{s=1}^{N}\sum_{i=0}^{3}\left\{(\hat{\theta}_{is} - \theta_{is}^*)\dot{\hat{\theta}}_{is} + \frac{\dot{\gamma}_s}{\underline{\gamma}} + \frac{\dot{\zeta}_s}{\underline{\zeta}}\right\} \qquad (16) \\
&\leq -\frac{1}{2}\boldsymbol{\xi}^T\mathbf{Q}_p\boldsymbol{\xi} - \mathbf{Y}_p^T(\hat{\boldsymbol{\Theta}}_p - \boldsymbol{\Theta}_p^*)||\mathbf{r}_p|| \\
&\quad + \sum_{s=1}^{N}\sum_{i=0}^{3}\left\{(\hat{\theta}_{is} - \theta_{is}^*)\dot{\hat{\theta}}_{is} + \frac{\dot{\gamma}_s}{\underline{\gamma}} + \frac{\dot{\zeta}_s}{\underline{\zeta}}\right\}. \qquad (17)
\end{aligned}$$

Using (9a)-(9b) we have

$$\begin{aligned}
\sum_{i=0}^{3}(\hat{\theta}_{ip} - \theta_{ip}^*)\dot{\hat{\theta}}_{ip} &= \sum_{j=0}^{2}(\hat{\theta}_{jp} - \theta_{jp}^*)(||\mathbf{r}_p||||\boldsymbol{\xi}||^j - \alpha_{jp}\hat{\theta}_{jp}) + (\hat{\theta}_{3p} - \theta_{3p}^*)(||\mathbf{r}_p||||\ddot{\bar{\mathbf{q}}}|| - \alpha_{3p}\hat{\theta}_{3p}) \\
&= \mathbf{Y}_p^T(\hat{\boldsymbol{\Theta}}_p - \boldsymbol{\Theta}_p^*)||\mathbf{r}_p|| + \sum_{i=0}^{3}\left\{\alpha_{ip}\hat{\theta}_{ip}\theta_{ip}^* - \alpha_{ip}\hat{\theta}_{ip}^2\right\}.
\end{aligned} \tag{18}$$

Similarly using the facts $\hat{\theta}_{is} \geq 0$, $0 < \underline{\zeta}_s \leq \zeta_s(t)$, $0 < \underline{\gamma}_s \leq \gamma_s(t)$ from (12) and $\underline{\zeta} = \min_{s\in\Omega}(\underline{\zeta}_s)$, $\underline{\gamma} = \min_{s\in\Omega}(\underline{\gamma}_s)$, (9c) and (9d) lead to

$$\begin{aligned}\frac{\dot{\zeta}_p}{\underline{\zeta}} &= -\left(1 + \hat{\theta}_{3p}||\ddot{\bar{\mathbf{q}}}|||\mathbf{r}_p||\right)\frac{\zeta_p}{\underline{\zeta}} + \frac{\bar{\epsilon}_p}{\underline{\zeta}} \\ &\leq -\hat{\theta}_{3p}||\ddot{\bar{\mathbf{q}}}|||\mathbf{r}_p|| + \frac{\bar{\epsilon}_p}{\underline{\zeta}}, \end{aligned} \tag{19}$$

$$\begin{aligned}\frac{\dot{\gamma}_{\bar{p}}}{\underline{\gamma}} &= -\left(1 + (\varrho_{\bar{p}}/2)\sum_{i=0}^{3}\hat{\theta}_{i\bar{p}}^2\right)\frac{\gamma_{\bar{p}}}{\underline{\gamma}} + \frac{\epsilon_{\bar{p}}}{\underline{\gamma}} \\ &\leq -\frac{\varrho_{\bar{p}}}{2}\sum_{i=0}^{3}\hat{\theta}_{i\bar{p}}^2 + \frac{\epsilon_{\bar{p}}}{\underline{\gamma}}, \end{aligned} \tag{20}$$

Substituting (18)-(20) in (17) yields

$$\begin{aligned}\dot{V} \leq &-\frac{1}{2}\lambda_{\min}(\mathbf{Q}_p)||\boldsymbol{\xi}||^2 + \sum_{i=0}^{3}\left\{\alpha_{ip}\hat{\theta}_{ip}\theta_{ip}^* - \bar{\alpha}_{ip}\hat{\theta}_{ip}^2\right\} \\ &+ \frac{\bar{\epsilon}_p}{\underline{\zeta}} - \left\{\sum_{\forall\bar{p}\in\Omega\setminus\{p\}}\sum_{i=0}^{3}\varrho_{\bar{p}}\hat{\theta}_{i\bar{p}}^2 - \frac{\epsilon_{\bar{p}}}{\underline{\gamma}}\right\}. \end{aligned} \tag{21}$$

Since $\hat{\theta}_{is} \geq 0$, $\zeta_s(t) \leq \bar{\zeta}_s$ and $\gamma_s(t) \leq \bar{\gamma}_s$ by design (12), one obtains

$$V \leq \frac{1}{2}\lambda_{\max}(\mathbf{P}_p)||\boldsymbol{\xi}||^2 + \sum_{s=1}^{N}\sum_{i=0}^{3}\frac{(\hat{\theta}_{is}^2 + \theta_{is}^{*\,2})}{2} + \frac{\bar{\gamma}_s}{\underline{\gamma}} + \frac{\bar{\zeta}_s}{\underline{\zeta}}. \tag{22}$$

Hence, using (22), the condition (21) is further simplified to

$$\begin{aligned}\dot{V} \leq &-\varrho V + \frac{\bar{\epsilon}_p}{\underline{\zeta}} + \sum_{i=0}^{3}\left\{\alpha_{ip}\hat{\theta}_{ip}\theta_{ip}^* - \bar{\alpha}_{ip}\hat{\theta}_{ip}^2\right\} \\ &+ \sum_{s=1}^{N}\sum_{i=0}^{3}\frac{\varrho_s\theta_{is}^{*\,2}}{2} + \varrho_s\left(\frac{\bar{\gamma}_s}{\underline{\gamma}} + \frac{\bar{\zeta}_s}{\underline{\zeta}}\right) + \frac{\epsilon_s}{\underline{\gamma}}, \end{aligned} \tag{23}$$

where $\varrho = \min_{p\in\Omega}\{\varrho_p\}$; $\bar{\alpha}_{ip} = (\alpha_{ip} - (\varrho_p/2)) > 0$ by design from (9e). Again, the following rearrangement can be made

$$\alpha_{ip}\hat{\theta}_{ip}\theta_{ip}^* - \bar{\alpha}_{ip}\hat{\theta}_{ip}^2 = -\bar{\alpha}_{ip}\left(\hat{\theta}_{ip} - \frac{\alpha_{ip}\theta_{ip}^*}{2\bar{\alpha}_{ip}}\right)^2 + \frac{\left(\alpha_{ip}\theta_{ip}^*\right)^2}{4\bar{\alpha}_{ip}}. \tag{24}$$

We had defined earlier $0 < \kappa < \varrho$. Then, using (24), $\dot{V}(t)$ from (23) gets simplified to

$$\dot{V}(t) \leq -\kappa V(t) - (\varrho - \kappa)V(t) + \delta, \tag{25}$$

where $\delta \triangleq \max_{p\in\Omega}\left(\sum_{i=0}^{3}\left(\alpha_{ip}\theta_{ip}^*\right)^2/(4\bar{\alpha}_{ip}) + (\bar{\epsilon}_p/\underline{\zeta})\right) + \sum_{s=1}^{N}\sum_{i=0}^{3}(\varrho_s/2)\theta_{is}^{*\,2} + (\varrho_s\bar{\gamma}_s)/\underline{\gamma} + (\varrho_s\bar{\zeta}_s)/\underline{\zeta} + (\epsilon_s/\underline{\gamma})$.

Case (ii) $||\mathbf{r}_\sigma|| < \varpi$

In this case, the time derivative of (13) yields

$$\begin{aligned}\dot{V} \leq &-\frac{1}{2}\boldsymbol{\xi}^T\mathbf{Q}_p\boldsymbol{\xi} + ||\chi_p||||\mathbf{r}_p|| - \rho_p\frac{||\mathbf{r}_p||^2}{\varpi} \\ &+ \sum_{s=1}^{N}\sum_{i=0}^{3}\left\{(\hat{\theta}_{is} - \theta_{is}^*)\dot{\hat{\theta}}_{is} + \frac{\dot{\gamma}_s}{\underline{\gamma}} + \frac{\dot{\zeta}_s}{\underline{\zeta}}\right\} \end{aligned} \tag{26}$$

$$\begin{aligned}\leq &-\frac{1}{2}\boldsymbol{\xi}^T\mathbf{Q}_p\boldsymbol{\xi} + ||\chi_p||||\mathbf{r}_p|| \\ &+ \sum_{s=1}^{N}\sum_{i=0}^{3}\left\{(\hat{\theta}_{is} - \theta_{is}^*)\dot{\hat{\theta}}_{is} + \frac{\dot{\gamma}_s}{\underline{\gamma}} + \frac{\dot{\zeta}_s}{\underline{\zeta}}\right\}. \end{aligned} \tag{27}$$

Following similar lines of proof as in Case (i) we have

$$\begin{aligned}\dot{V} &\leq -\kappa V - (\varrho - \kappa)V + \delta + (\mathbf{Y}_p^T\hat{\mathbf{\Theta}}_p - \hat{\theta}_{3p}||\ddot{\bar{\mathbf{q}}}||)||\mathbf{r}_p|| \\ &= -\kappa V - (\varrho - \kappa)V + \delta + \sum_{j=0}^{2}\hat{\theta}_{jp}||\boldsymbol{\xi}||^j||\mathbf{r}_p||. \end{aligned} \tag{28}$$

From (4) one can verify $||\mathbf{r}|| < \varphi \Rightarrow ||\boldsymbol{\xi}|| \in \mathcal{L}_\infty$ and consequently, the adaptive law (9a) implies $||\mathbf{r}||, ||\boldsymbol{\xi}|| \in \mathcal{L}_\infty \Rightarrow \hat{\theta}_{jp}(t) \in \mathcal{L}_\infty$, $j = 0, 1, 2$. Therefore, $\exists\delta_1 \in \mathbb{R}^+$ such that $\sum_{j=0}^{2}\hat{\theta}_{jp}||\boldsymbol{\xi}||^j \leq \delta_1\ \forall p \in \Omega$ when $||\mathbf{r}_p|| < \varphi$. Hence, replacing this relation in (28) yields

$$\dot{V}(t) \leq -\kappa V(t) - (\varrho - \kappa)V(t) + \delta + \varpi\delta_1. \tag{29}$$

Therefore, investigating the stability results of Cases (i) and (ii), it can be concluded that $\dot{V}(t) \leq -\varrho V(t)$ when

$$V(t) \geq \mathcal{B} \triangleq \frac{\delta + \varpi\delta_1}{(\varrho - \kappa)}. \tag{30}$$

In light of this, further analysis is needed to observe the behaviour of $V(t)$ between the two consecutive switching instants, i.e., $t \in [t_l\ t_{l+1})$, for two possible scenarios:

(i) when $V(t) \geq \mathcal{B}$, we have $\dot{V}(t) \leq -\varrho V(t)$ implying exponential decrease of $V(t)$;

(ii) when $V(t) < \mathcal{B}$, no exponential decrease can be derived.

Behaviour of $V(t)$ is discussed below individually for these two scenarios.

Scenario (i): There exists a time, call it T_1, when $V(t)$ enters into the bound $\mathcal{B}$ and $N_\sigma(t)$ denotes the number of all switching intervals for $t \in [t_0\ \ t_0 + T_1)$. Accordingly, for $t \in [t_0\ \ t_0 + T_1)$, using (15) and $N_\sigma(t_0, t)$ from Definition 1 we have

$$\begin{aligned} V(t) &\leq \exp\left(-\kappa(t - t_{N_\sigma(t)-1})\right) V(t_{N_\sigma(t)-1}) \\ &\leq \mu\exp\left(-\kappa(t - t_{N_\sigma(t)-1})\right) V(t^-_{N_\sigma(t)-1}) \\ &\leq \mu\exp\left(-\kappa(t - t_{N_\sigma(t)-1})\right) \\ &\quad \cdot \mu\exp\left(-\kappa(t_{N_\sigma(t)-1} - t_{N_\sigma(t)-2})\right) V(t^-_{N_\sigma(t)-2}) \\ &\qquad\qquad \vdots \\ &\leq \mu\exp\left(-\kappa(t - t_{N_\sigma(t)-1})\right) \mu\exp\left(-\kappa(t_{N_\sigma(t)-1} - t_{N_\sigma(t)-2})\right) \\ &\quad \cdots \mu\exp\left(-\kappa(t_1 - t_0)\right) V(t_0) \\ &= \mu^{N_\sigma(t_0,t)}\exp\left(-\kappa(t - t_0)\right) V(t_0) \\ &= c\left(\exp\left(-\kappa + (\ln\mu/\vartheta)\right)\right) V(t_0), \end{aligned} \tag{31}$$

where $c \triangleq \exp\left(N_0 \ln\mu\right)$ is a constant. Substituting the ADT condition $\vartheta > \ln\mu/\varrho$ in (31) yields $V(t) < cV(t_0)$ for $t \in [t_0\ \ t_0 + T_1)$. Moreover, as $V(t_0 + T_1) < \mathcal{B}$, one has $V(t_{N_\sigma(t)+1}) < \mu\mathcal{B}$ from (15) at the next switching instant $t_{N_\sigma(t)+1}$ after $t_0 + T_1$. This implies that $V(t)$ may be larger than $\mathcal{B}$ from the instant $t_{N_\sigma(t)+1}$. This necessitates further analysis.

We assume $V(t) \geq \mathcal{B}$ for $t \in [t_{N_\sigma(t)+1}\ \ t_0 + T_2)$, where T_2 denotes the time before next switching. Let $\bar{N}_\sigma(t)$ represents the number of all switching intervals for $t \in [t_{N_\sigma(t)+1}\ \ t_0 + T_2)$. Then, substituting $V(t_0)$ with $V(t_{N_\sigma(t)+1})$ in (31) and following the similar procedure for analysis as (31), we have $V(t) \leq cV(t_{N_\sigma(t)+1}) < c\mu\mathcal{B}$ for $t \in [t_{N_\sigma(t)+1}\ \ t_0 + T_2)$. Since $V(t_0 + T_2) < \mathcal{B}$, we have $V(t_{N_\sigma(t)+\bar{N}_\sigma(t)+2}) < \mu\mathcal{B}$ at the next switching instant $t_{N_\sigma(t)+\bar{N}_\sigma(t)+2}$ after $t_0 + T_2$. If we follow similar lines of proof recursively, we can come to the conclusion that $V(t) < c\mu\mathcal{B}$ for $t \in [t_0 + T_1\ \ \infty)$. This confirms that once $V(t)$ enters the interval $[0, \mathcal{B}]$, it cannot exceed the bound $c\mu\mathcal{B}$ any time later with the ADT switching law (10).

Scenario (ii): It can be verified that the same argument below (31) also holds for Scenario (ii).

Thus, observing the stability arguments of the Scenarios (i) and (ii), it can be concluded that the closed-loop system remains UUB with the control laws (5) and (8) with the adaptive law (9) and switching law (10) implying

$$V(t) \leq \max\left(cV(t_0), c\mu\mathcal{B}\right),\ \ \forall t \geq t_0. \tag{32}$$

Again, the definition of the Lyapunov function (13) yields

$$V(t) \geq (1/2)\lambda_{\min}(\mathbf{P}_{\sigma(t)})||\boldsymbol{\xi}||^2 \geq \left(\underline{\varrho}_m/2\right)||\boldsymbol{\xi}||^2. \tag{33}$$

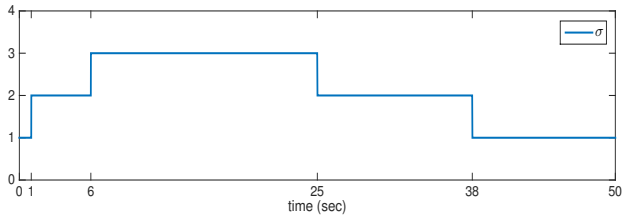

FIGURE 3 The switching signal.

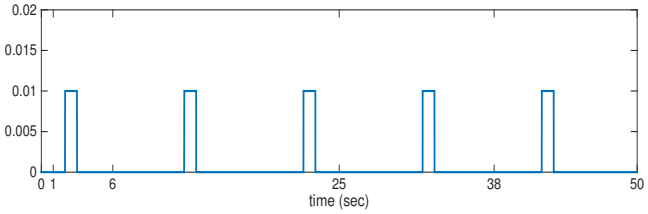

FIGURE 4 Pulse type disturbance.

Using (32) and (33) we have

$$||\boldsymbol{\xi}||^2 \leq \left(2/\underline{\varrho}_m\right) \max\left(cV(t_0), c\mu\mathcal{B}\right), \quad \forall t \geq t_0. \tag{34}$$

Therefore, using the expression of $\mathcal{B}$ from (22), an ultimate bound b on the tracking error $\boldsymbol{\xi}$ can be found as (11). □

Note that in collocated design, it is standard to consider the internal dynamics to be stable/bounded a priori[26,27]. In the following, a few design aspects of the proposed mechanism are highlighted.

Remark 5. (The role of gain $\mathbf{D}_\sigma$ and its selection). The control law (5a) relies on the inverse dynamics-type design: in its absence, $\mathbf{D}_\sigma$ would have been replaced by some nominal value of mass matrix following the conventional design (cf.[23,36]). However, according to Remark 1, such knowledge is unavailable. Again, avoiding inverse dynamics-type design and involving mass matrix in the Lyapunov function eventually lead to a switching law that relies on bound knowledge of mass matrix[22]. These observations highlight the role of $\mathbf{D}_\sigma$ to realize a switched controller without any knowledge of mass matrix.

Aside being positive definite, the proposed design does not put any restriction on the choice of $\mathbf{D}_\sigma$. It can be observed from (6) that higher values of $\mathbf{D}_\sigma$ reduces the effect of uncertainty $\boldsymbol{\chi}_\sigma$ on the error dynamics, albeit at the cost of higher control input (cf. (5a)). Therefore, $\mathbf{D}_\sigma$ needs to be designed according to the application requirements.

5 | SIMULATION RESULTS

We test the proposed controller for a switched dynamics scenario as in Fig. 1 having three phases (a.k.a subsystems), denoted by $\sigma = 1, 2, 3$. For fruitful verification and as found in many applications (cf.[37,38]), we verify the controller on the six degrees-of-freedom underactuated quadrotor model as in Appendix (cf. (A1)). The following parametric variations (due to addition of payload) are selected for different subsystems

$$\begin{aligned}
\sigma = 1 &: \; m = 1.5,\; I_{xx} = I_{yy} = 1.69 \cdot 10^{-5},\; I_{zz} = 3.38 \cdot 10^{-5},\\
\sigma = 2 &: \; m = 1.6,\; I_{xx} = 0.011,\; I_{yy} = 0.010,\; I_{zz} = 1.27 \cdot 10^{-4},\\
\sigma = 3 &: \; m = 1.7,\; I_{xx} = 0.032,\; I_{yy} = 0.030,\; I_{zz} = 2.20 \cdot 10^{-4}.
\end{aligned}$$

The objective for the quadrotor is to lift and drop various payloads at different heights while starting from the ground position. To achieve this task, the following desired trajectories are defined $x^d = y^d = 0, z^d = 2 + \sin(0.1t), \phi^d = \varphi^d = \psi^d = 0$ with an initial position of $x(0) = y(0) = 0.1, z(0) = 0, \phi(0) = \varphi(0), \psi(0) = 0.1$. Selection of $\mathbf{K}_{11} = 120\mathbf{I}, \mathbf{K}_{21} = 100\mathbf{I}, \mathbf{K}_{12} = 150\mathbf{I}, \mathbf{K}_{22} = 120\mathbf{I}, \mathbf{K}_{13} = 200\mathbf{I}, \mathbf{K}_{23} = 140\mathbf{I}, \mathbf{Q}_1 = \mathbf{Q}_2 = \mathbf{Q}_3 = 2\mathbf{I}$, $\kappa = 0.9\varrho$ yields the ADT $\vartheta^* = 6.57$sec according to (10).

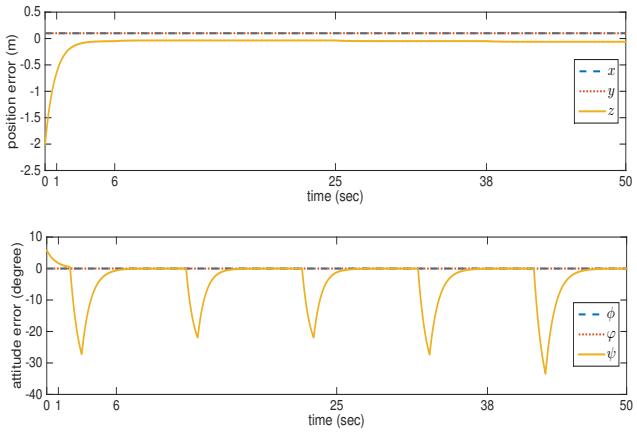

FIGURE 5 Tracking performance of the proposed controller.

Therefore, a switching law $\sigma(t)$ is designed as in Fig. 3 (note that the initial fast switchings are compensated by slower switchings later on).

Other control parameters are designed as

$$\mathbf{D}_\sigma = \begin{bmatrix} 2 & 0 & 0 & 0 \\ 0 & 1\cdot 10^{-4} & 0 & 0 \\ 0 & 0 & 1\cdot 10^{-4} & 0 \\ 0 & 0 & 0 & 1\cdot 10^{-4} \end{bmatrix},$$

$\alpha_{i\sigma} = 0.6, \epsilon_\sigma = \bar{\epsilon}_\sigma = 0.005$ with $i = 0, 1, 2, 3$ for all σ. The initial conditions are selected as $\hat{\theta}_{0\sigma}(0) = 1.2, \hat{\theta}_{1\sigma}(0) = 1.3, \hat{\theta}_{2\sigma}(0) = 1.4, \hat{\theta}_{3\sigma}(0) = 1.5, \zeta_\sigma(0) = \gamma_\sigma(0) = 1\ \forall\sigma$. The external disturbance is selected as $\mathbf{d}_\sigma = \{0.05\sin(0.5t), 0, 0, d_p\}\ \forall\sigma$, where d_p represents a pulse type disturbance (cf. Fig. 4) emulating sudden disturbances like gust of wind. It is worth remarking here that, the proposed mechanism being a collocated one, external disturbances should be selected such that the nonactuated dynamics does not become unstable (cf.[26,27]). Therefore, no external disturbances are considered in (ϕ, φ) as well as in (x, y).

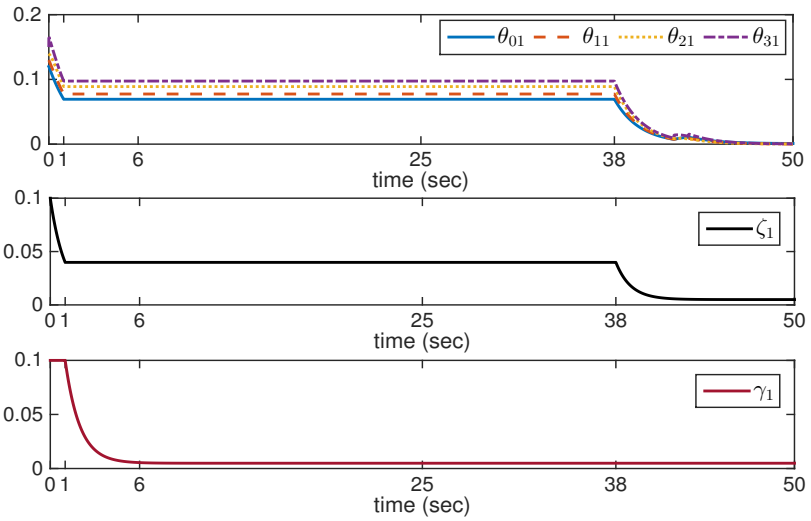

FIGURE 6 Gains for subsystem 1.

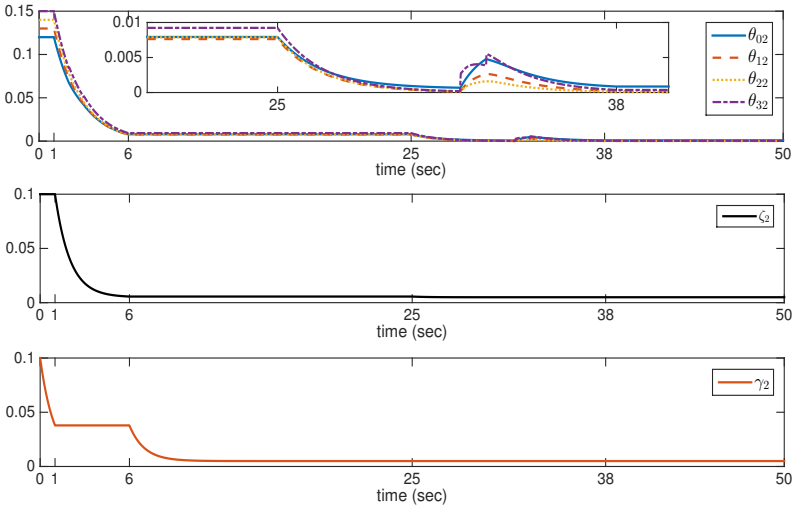

FIGURE 7 Gains for subsystem 2.

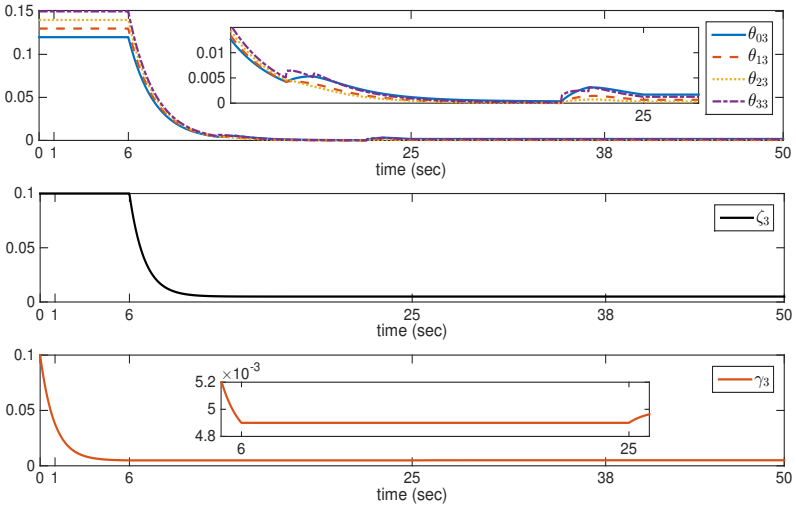

FIGURE 8 Gains for subsystem 3.

The performance of the proposed controller is depicted in Fig. 5 in terms of tracking errors, where the attitude errors are reported in degree for better comprehension. In line with the proposed adaptive law (9a)-(9d), Figs. 6-8 reveal that: (i) for an active subsystem, only the gains $\hat{\theta}_{ip}$ and ζ_p are updated while γ_p remains constant; (ii) for an inactive subsystem, while $\gamma_{\bar{p}}$ is updated, $\hat{\theta}_{i\bar{p}}$ and $\zeta_{\bar{p}}$ remain constant.

6 | CONCLUSIONS

A new concept of adaptive control design for quadrotor was introduced for vertical operations, using the framework of average dwell time based switched dynamics. The proposed design did not require any a priori knowledge of structure and bound of uncertainty. The effectiveness of the concept was validated via simulations with dynamically varying payload.

□

APPENDIX

A DYNAMICS OF QUADROTOR

The dynamics of a six degrees-of-freedom quadrotor in Earth-fixed coordinated frame is given by[3,7]

$$m\begin{bmatrix}\ddot{x}\\ \ddot{y}\\ \ddot{z}\end{bmatrix}+\begin{bmatrix}0\\0\\mg\end{bmatrix}=\mathbf{R}^T\begin{bmatrix}0\\0\\T_{th},\end{bmatrix} \tag{A1a}$$

$$\begin{aligned}&\frac{I_{xx}}{l}\ddot{\phi}+\frac{I_{zz}-I_{yy}}{l}\dot{\varphi}\dot{\psi}=\tau_{\phi},\\ &\frac{I_{yy}}{l}\ddot{\varphi}+\frac{I_{xx}-I_{zz}}{l}\dot{\phi}\dot{\psi}=\tau_{\varphi},\\ &I_{zz}\ddot{\psi}+(I_{yy}-I_{xx})\dot{\varphi}\dot{\phi}=\tau_{\psi},\end{aligned} \tag{A1b}$$

where

$$\mathbf{R}=\begin{bmatrix}c_\psi c_\varphi & s_\psi c_\varphi & -s_\varphi\\ c_\psi s_\varphi s_\phi - s_\psi c_\phi & s_\psi s_\varphi s_\phi + c_\psi c_\phi & s_\phi c_\varphi\\ c_\psi s_\varphi c_\phi + s_\psi s_\phi & s_\psi s_\varphi c_\phi - c_\psi s_\phi & c_\varphi c_\phi\end{bmatrix}$$

is an orthogonal rotational matrix and $c_{(\cdot)}, s_{(\cdot)}$ denote $\cos(\cdot), \sin(\cdot)$; m is the mass of the overall system; l is arm-length of the rotor units; I_{xx}, I_{yy}, I_{zz} are the inertia terms in x, y and z directions respectively; T_{th} is the total thrust and $\tau_{(\cdot)}$ is the moment in the direction of $(\cdot)$.

Multiplying both side of the position subsystem (A1a) with $\mathbf{R}$ yields

$$m\ddot{x}c_\psi c_\varphi + m\ddot{y}s_\psi c_\varphi - m\ddot{z}s_\varphi - mgs_\varphi = 0, \tag{A2a}$$

$$m\ddot{x}(c_\psi s_\varphi s_\phi - s_\psi c_\phi) + m\ddot{y}(s_\psi s_\varphi s_\phi + c_\psi c_\phi) + m\ddot{z}s_\phi c_\varphi + mgs_\phi c_\varphi = 0, \tag{A2b}$$

$$m\ddot{x}(c_\psi s_\varphi c_\phi + s_\psi s_\phi) + m\ddot{y}(s_\psi s_\varphi c_\phi - c_\psi s_\phi) + m\ddot{z}c_\varphi c_\phi + mgc_\varphi c_\phi = T_{th}. \tag{A2c}$$

Remark 6. The above mathematical arrangement helps to avoid singularity while computing T_{th} and consequently avoids any a priori boundedness assumption on ϕ and φ as in[8].

After such rearrangements of the dynamics, we are now ready to define the (non-switched) four degrees-of-freedom dynamics structure suitable for collocated design as

$$\mathbf{M}(\mathbf{q})\ddot{\mathbf{q}} + \mathbf{C}(\mathbf{q},\dot{\mathbf{q}})\dot{\mathbf{q}} + \mathbf{G}(\mathbf{q}) + \mathbf{H}(\mathbf{q})\ddot{\mathbf{q}}_{\mathbf{u}} = \boldsymbol{\tau}, \tag{A3}$$

where

$$\mathbf{M}=\begin{bmatrix}m(c_\varphi c_\phi) & 0 & 0 & 0\\ 0 & \frac{I_{xx}}{l} & 0 & 0\\ 0 & 0 & \frac{I_{yy}}{l} & 0\\ 0 & 0 & 0 & I_{zz}\end{bmatrix},\ \mathbf{G}=\begin{bmatrix}mg(c_\varphi c_\phi)\\0\\0\\0\end{bmatrix}$$

$$\mathbf{C}=\begin{bmatrix}0 & 0 & 0 & 0\\ 0 & 0 & 0 & \frac{(I_{zz}-I_{yy})}{l}\dot{\varphi}\\ 0 & \frac{(I_{xx}-I_{zz})}{l}\dot{\psi} & 0 & 0\\ 0 & 0 & (I_{yy}-I_{xx})\dot{\phi} & 0\end{bmatrix},$$

$$\mathbf{H}=\begin{bmatrix}m(c_\psi s_\varphi c_\phi + s_\psi s_\phi) & m(s_\psi s_\varphi c_\phi - c_\psi s_\phi)\\ 0 & 0\\ 0 & 0\\ 0 & 0\end{bmatrix},$$

$$\boldsymbol{\tau}=\begin{bmatrix}T_{th}\\ \tau_\phi\\ \tau_\varphi\\ \tau_\psi\end{bmatrix},\ \mathbf{q}=\begin{bmatrix}z\\ \phi\\ \varphi\\ \psi\end{bmatrix},\ \mathbf{q}_{\mathbf{u}}=\begin{bmatrix}x\\ y\end{bmatrix}.$$

References

1. Du Y, Fang J, Miao C. Frequency-domain system identification of an unmanned helicopter based on an adaptive genetic algorithm. *IEEE Transactions on Industrial Electronics* 2013; 61(2): 870–881.

2. Lugo JJ, Zell A. Framework for autonomous on-board navigation with the AR. Drone. *Journal of Intelligent & Robotic Systems* 2014; 73(1-4): 401–412.

3. Tang S, Kumar V. Mixed integer quadratic program trajectory generation for a quadrotor with a cable-suspended payload. *IEEE International Conference on Robotics and Automation (ICRA)* 2015: 2216–2222.

4. Yang S, Xian B. Energy-based Nonlinear Adaptive Control Design for the Quadrotor UAV System with a Suspended Payload. *IEEE Transactions on Industrial Electronics* 2019.

5. Liberzon D. *Switching in systems and control*. Springer Science & Business Media . 2003.

6. Rubí B, Pérez R, Morcego B. A Survey of Path Following Control Strategies for UAVs Focused on Quadrotors. *Journal of Intelligent & Robotic Systems*: 1–25.

7. Nicol C, Macnab C, Ramirez-Serrano A. Robust adaptive control of a quadrotor helicopter. *Mechatronics* 2011; 21(6): 927–938.

8. Bialy BJ, Klotz J, Brink K, Dixon WE. Lyapunov-based robust adaptive control of a quadrotor UAV in the presence of modeling uncertainties. *American Control Conference* 2013: 13–18.

9. Dydek ZT, Annaswamy AM, Lavretsky E. Adaptive control of quadrotor UAVs: A design trade study with flight evaluations. *IEEE Transactions on control systems technology* 2012; 21(4): 1400–1406.

10. Ha C, Zuo Z, Choi FB, Lee D. Passivity-based adaptive backstepping control of quadrotor-type UAVs. *Robotics and Autonomous Systems* 2014; 62(9): 1305–1315.

11. Mofid O, Mobayen S. Adaptive sliding mode control for finite-time stability of quad-rotor UAVs with parametric uncertainties. *ISA transactions* 2018; 72: 1–14.

12. Tran TT, Ge SS, He W. Adaptive control of a quadrotor aerial vehicle with input constraints and uncertain parameters. *International Journal of Control* 2018; 91(5): 1140–1160.

13. Tian B, Cui J, Lu H, Zuo Z, Zong Q. Adaptive finite-time attitude tracking of quadrotors with experiments and comparisons. *IEEE Transactions on Industrial Electronics* 2019.

14. Zhao B, Xian B, Zhang Y, Zhang X. Nonlinear robust adaptive tracking control of a quadrotor UAV via immersion and invariance methodology. *IEEE Transactions on Industrial Electronics* 2014; 62(5): 2891–2902.

15. Lai G, Liu Z, Zhang Y, Chen CP, Xie S. Adaptive backstepping-based tracking control of a class of uncertain switched nonlinear systems. *Automatica* 2018; 91: 301–310.

16. Yuan S, De Schutter B, Baldi S. Robust adaptive tracking control of uncertain slowly switched linear systems. *Nonlinear Analysis: Hybrid Systems* 2018; 27: 1–12.

17. Yuan S, Zhang F, Baldi S. Adaptive tracking of switched nonlinear systems with prescribed performance using a reference-dependent reparametrisation approach. *International Journal of Control* 2019; 92(6): 1243–1251.

18. Lou ZE, Zhao J. Immersion-and invariance-based adaptive stabilization of switched nonlinear systems. *International Journal of Robust and Nonlinear Control* 2018; 28(1): 197–212.

19. Chen W, Wen C, Wu J. Global Exponential/Finite-Time Stability of Nonlinear Adaptive Switching Systems with Applications in Controlling Systems with Unknown Control Direction. *IEEE Transactions on Automatic Control* 2018.

20. Yuan S, Zhang L, Holub O, Baldi S. Switched Adaptive Control of Air Handling Units With Discrete and Saturated Actuators. *IEEE Control Systems Letters* 2018; 2(3): 417-422.

21. Yuan S, De Schutter B, Baldi S. Adaptive Asymptotic Tracking Control of Uncertain Time-Driven Switched Linear Systems. *IEEE Transactions on Automatic Control* 2017; 62(11): 5802-5807.

22. Roy S, Baldi S. On reduced-complexity robust adaptive control of switched Euler–Lagrange systems. *Nonlinear Analysis: Hybrid Systems* 2019; 34: 226–237.

23. Roy S, Baldi S. A Simultaneous Adaptation Law for a Class of Nonlinearly Parametrized Switched Systems. *IEEE Control Systems Letters* 2019; 3(3): 487–492.

24. Hespanha JP, Morse AS. Stability of switched systems with average dwell-time. *Proceedings of the 38th IEEE Conference on Decision and Control* 1999: 2655–2660.

25. Spong MW, Vidyasagar M. *Robot dynamics and control*. John Wiley & Sons . 2008.

26. Shkolnik A, Tedrake R. High-dimensional underactuated motion planning via task space control. *IEEE/RSJ International Conference on Intelligent Robots and Systems* 2008: 3762–3768.

27. Spong MW. Partial feedback linearization of underactuated mechanical systems. *IEEE/RSJ International Conference on Intelligent Robots and Systems* 1994: 314–321.

28. Roy S, Baldi S. Towards structure-independent stabilization for uncertain underactuated Euler–Lagrange systems. *Automatica* 2020; 113: 108775.

29. Roy S, Kar IN, Lee J, Jin M. Adaptive-robust time-delay control for a class of uncertain Euler–Lagrange systems. *IEEE Transactions on Industrial Electronics* 2017; 64(9): 7109–7119.

30. Spong MW, Ortega R. On adaptive inverse dynamics control of rigid robots. *IEEE Transactions on Automatic Control* 1990; 35(1): 92–95.

31. Roy S, Baldi S, Fridman LM. On adaptive sliding mode control without a priori bounded uncertainty. *Automatica* 2019: 108650.

32. Roy S, Kar IN. *Adaptive-Robust Control with Limited Knowledge on Systems Dynamics: An Artificial Input Delay Approach and Beyond*. 257. Springer Nature . 2019.

33. Lee J, Yoo C, Park YS, et al. An experimental study on time delay control of actuation system of tilt rotor unmanned aerial vehicle. *Mechatronics* 2012; 22(2): 184–194.

34. Roy S, Lee J, Baldi S. A new continuous-time stability perspective of time-delay control: Introducing a state-dependent upper bound structure. *IEEE Control Systems Letters* 2019; 3(2): 475–480.

35. Roy S, Lee J, Baldi S. A New Adaptive-Robust Design for Time Delay Control under State-dependent Stability Condition. *IEEE Transactions on Control Systems Technology* 2020.

36. Roy S, Roy SB, Lee J, Baldi S. Overcoming the underestimation and overestimation problems in adaptive sliding mode control. *IEEE/ASME Transactions on Mechatronics* 2019; 24(5): 2031–2039.

37. Ye J, Roy S, Godjevac M, Baldi S. Observer-based robust control for dynamic positioning of large-scale heavy lift vessels. *IFAC-PapersOnLine* 2019; 52(3): 138–143.

38. Roy S, Patel A, Kar IN. Analysis and Design of a Wide-Area Damping Controller for Inter-Area Oscillation With Artificially Induced Time Delay. *IEEE Transactions on Smart Grid* 2019; 10(4): 3654–3663.